PROCEEDINGS OF SPIE

SPIEDigitalLibrary.org/conference-proceedings-of-spie

Noninvasive point-of-care measurement of gastrointestinal permeability

Richard B. Dorshow, J. R. Johnson, Martin P. Debreczeny, I. Rochelle Riley, Jeng-Jong Shieh, et al.

Richard B. Dorshow, J. R. Johnson, Martin P. Debreczeny, I. Rochelle Riley, Jeng-Jong Shieh, Thomas E. Rogers, Carla Hall-Moore, Nurmohammad Shaikh, Phillip I. Tarr, "Noninvasive point-of-care measurement of gastrointestinal permeability ," Proc. SPIE 10893, Reporters, Markers, Dyes, Nanoparticles, and Molecular Probes for Biomedical Applications XI, 1089307 (7 March 2019); doi: 10.1117/12.2507965

SPIE.

Event: SPIE BiOS, 2019, San Francisco, California, United States

Noninvasive point-of-care measurement of gastrointestinal permeability

Richard B. Dorshow,[1,*] J.R. Johnson,[1] Martin P. Debreczeny,[1] I. Rochelle Riley,[1] Jeng-Jong Shieh,[1] Thomas E. Rogers,[1] Carla Hall-Moore,[2] Nurmohammad Shaikh,[2] and Phillip I. Tarr[2]

[1]MediBeacon Inc., 1100 Corporate Square Drive, St. Louis, MO 63132, USA

[2]Department of Pediatrics, Washington University School of Medicine, St. Louis, MO 63110, USA

ABSTRACT

The intestinal mucosal barrier prevents macromolecules and pathogens from entering the circulatory stream in a healthy gut. Tight junctions in this barrier are compromised in many intestinal disorders including inflammatory bowel diseases (such as Crohn's and ulcerative colitis), celiac disease, graft vs host disease, environmental enteropathy, and enteric dysfunction. Dual sugar absorption tests are a standard method for measuring gastrointestinal integrity in humans. The larger molecular weight sugar, lactulose, is minimally absorbed through a healthy gut. The smaller molecular weight sugar, mannitol or rhamnose, in contrast, is readily absorbed through both a healthy and inflamed gut. Thus, a higher ratio of lactulose to mannitol or rhamnose reflects increased intestinal permeability. However, several issues prevent the widespread use of the dual sugar assay including requirements for lengthy urine collection, transport of specimens under conditions free from contamination and bacterial growth, analysis by sophisticated laboratory equipment, and the associated lengthy turnaround time. In a recent publication, the feasibility of employing a dual fluorescent tracer agent assay to mimic the dual sugar absorption test without the need for specimen collection was reported. This dual fluorophore assay for GI permeability was demonstrated in an indomethacin-induced bowel disease model in rats. However, one of the fluorophores was not entirely biocompatible. Herein is reported a dual fluorophore system that is totally biocompatible, with emphasis on the transdermal detection of the fluorophores, thus enabling the use of the technology for noninvasive point-of-care gastrointestinal permeability determination.

KEYWORDS

gastrointestinal permeability**,** fluorescence tracer agent, dual sugar absorption test, enteropathy, point-of-care measurement

1. INTRODUCTION

Maintaining intestinal inter-cellular integrity is a cardinal function of a healthy gut. Intestinal permeability is increased in multiple intestinal disorders, including Crohn's Disease, ulcerative colitis, celiac disease, and graft-vs.- host disease, as well as in extra-intestinal disorders such as types I and II diabetes, non-alcoholic fatty liver disease, and juvenile inflammatory arthritidies.[1-5]

Reporters, Markers, Dyes, Nanoparticles, and Molecular Probes for Biomedical Applications XI, edited by Samuel Achilefu, Ramesh Raghavachari, Proc. of SPIE Vol. 10893, 1089307 · © 2019 SPIE
CCC code: 1605-7422/19/$18 · doi: 10.1117/12.2507965

Generally, intestinal permeability in humans has been determined using the dual sugar absorption test (DSAT), where patients drink a solution containing a disaccharide, usually lactulose (MW=342), and a monosaccharide, either mannitol (MW=182) or rhamnose (MW=164). These molecules enter the bloodstream from the gut and are excreted intact in urine. The urinary ratios of lactulose to mannitol, or lactulose to rhamnose indicate the degree of intestinal permeability, with increased permeability characterized by an elevated ratio, reflecting the heavier disaccharide entering into circulation.[6-9]

These dual sugar absorption tests are theoretically sound, but their utility is diminished by the need to collect urine, transport the urine (preserved and frozen) to central testing facilities, and quality control challenges at the point of assay with the needed sophisticated laboratory instrumentation.[10] We recently presented data on two orally-administered fluorescent tracer agents (chosen from our portfolio of renal-excreted dyes) of molecular weights similar to the usual dual sugars, and compared the DSAT ratios in a rat indomethacin challenge model.[11] These fluorophores have the added attribute of transdermal detection in real-time, at the point-of-care. This allows for a specimen-free measurement, overcoming the DSAT's detrimental aspects. The report herein employs a new fluorophore as the larger molecular weight entity, such that both fluorophores are completely water soluble and biocompatible. We especially focus on the transdermal measurements and show that these can distinguish between a normal gut and a diseased gut in the indomethacin disease-induced rat model.

2. METHODS AND MATERIALS

2.1 Fluorophores

The two fluorophores in this study, both belonging to the pyrazine class, were chosen to approximately match the molecular weights of the dual sugar combination lactulose and mannitol. The structures are shown in Figure 1.

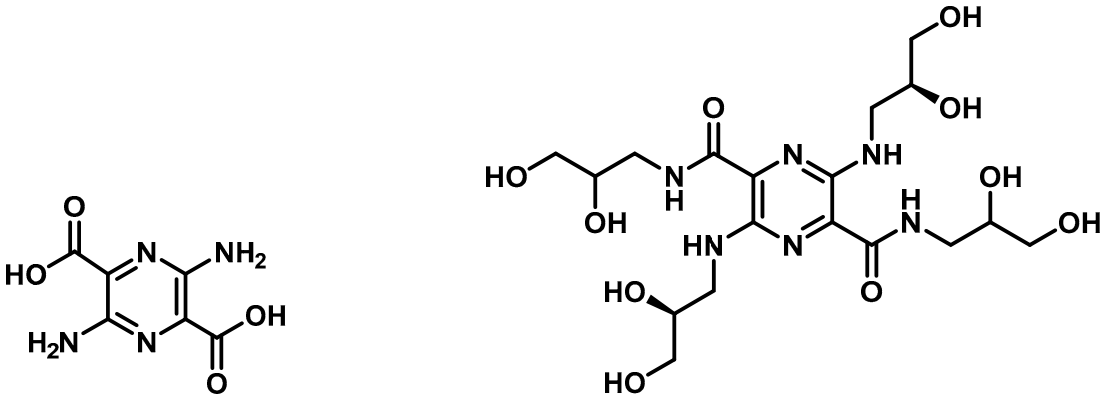

Figure 1: MB-301 (left) and MB-404 (right) structural diagrams.

MB-301 (3,6-diaminopyrazine-2,5-dicarboxylic acid) has a molecular weight of 198, with light absorption and emission maxima at wavelengths 405 nm and 540 nm, respectively.[12]

MB-404 (N2,N5-bis(2,3-dihydroxypropyl)-3,6-bis(((S)-2,3-dihydroxypropyl)amino)pyrazine-2,5-dicarboxamide) has a molecular weight of 492, with light absorption and emission maxima at wavelengths 500 nm and 620 nm, respectively. In animal experiments, this compound is excreted almost entirely by the renal system, with negligible protein binding.[13]

2.2 Animal preparation and experimental set-up

2.2.1 Day prior to experiment

The procedure for administering indomethacin, which causes the gut lesion and hence dysfunction, to the rats, as well as the procedure for administration of the vehicle is as follows. One day prior to tracer administration, female Sprague-Dawley rats were challenged with indomethacin (15 mg/kg), or with vehicle (2% methylcellulose in water).

Following the challenge, a 2.5 x 2.5 cm area on the anterior section of each animal's back was shaved and treated with depilating cream, necessary for the transdermal experiments described below.

2.2.2 Day of experiment:

Anesthesia set up: Immediately before experiments, animals were anesthetized with 1.5% isoflurane, and a catheter inserted into their urinary bladder. The gavage mixture was prepared consisting of MB-404 (45.77 mg/mL) and MB-301 (8.0 mg/mL), and administered at 2 mL/kg (i.e., 91.5 mg/kg MB-404 and 16 mg/kg MB-301).

2.2.3 Experimental Procedure

Animals were placed on their belly and the depilated area was wiped with a ChloraPrep One-Step (CareFusion, 260299) skin prep applicator, followed by wiping with a Cavilon (3M 3344) applicator. A 2.5 x 2.5 cm medical adhesive (3M 1577) was placed over this prepped area. A bifurcated fiber optic bundle for light excitation delivery and fluorescence emission collection, outfitted with a Vascular Access Harness™ (Instech Labs CIH105), was gently placed against shaved area.

Transdermal fluorescence detection was initiated, and baseline fluorescence was acquired for 10 minutes. The animals were then removed from the anesthesia holder for vertical gavage with the fiber optic bundle remaining attached. The animals were placed into the anesthesia manifold following sequential gavage.

Figure 2. Animal experimental set-up during transdermal fluorescence readout.

2.3 Transdermal Fluorescence Instrumentation

A dual-wavelength transdermal fluorescence detection system was constructed to simultaneously monitor MB-301 and MB-404 *in vivo*. The system consists of four identical channels (probes), enabling simultaneous monitoring of up to four animals. Figure 3 shows a schematic diagram of the illumination system, and one probe.

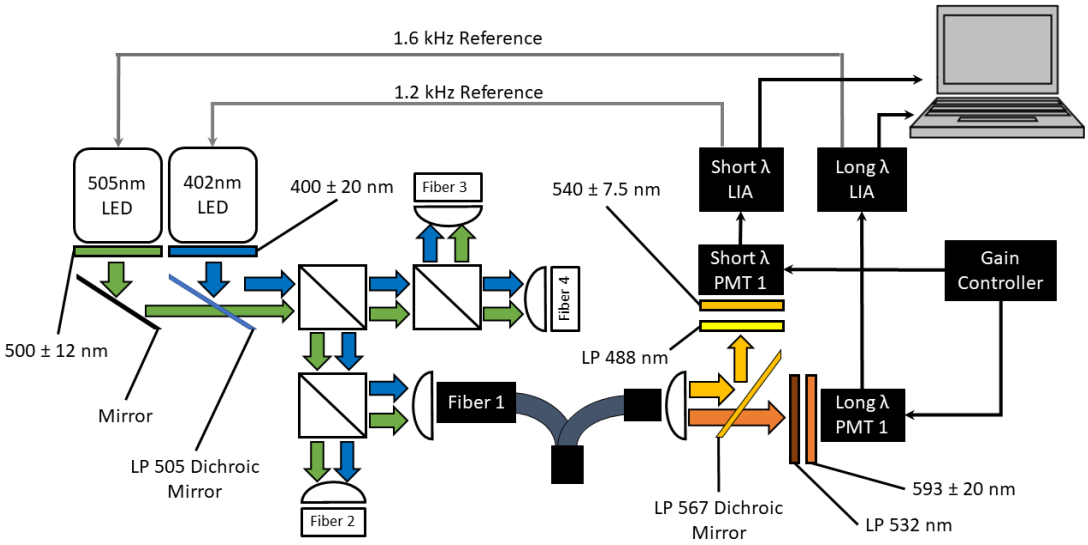

Figure 3: Transdermal fluorescence detection system schematic illustrating the illumination system and one of four identical detection channels.

The illumination source uses a 402 and a 505 nm light-emitting diode (LED) (Lightspeed Technologies Inc., Model LEDH-402 and LEDH-505), each packaged in a driver with integrated optics (Lightspeed Technologies Inc., Model HPLS-36AD3500). LED emission was collimated (Lightspeed Technologies Inc., Model OH36-24 x 11) before passing through a 40 nm single bandpass filter centered at 400 nm (Semrock FF01-400/40-25) or a 24 nm single bandpass filter centered at 500 nm (Semrock FF01-500/24-25). The LED output was then diverted 90˚ into a 50:50 beam splitter via a standard mirror (505 nm LED) or a 505 nm long pass dichroic mirror (ThorLabs DMLP505R) (402 nm LED). The resulting LED outputs were split again via two 50:50 beam splitters resulting in four equal dual-wavelength light sources. Each resulting output was focused onto one end of a bifurcated fiber bundle (Oriel 77565). Fiber bundles consisted of a randomly-mixed, close-packed array of source and detection fibers (individual fiber diameter: 55 µm, 0.56 NA, common bundle diameter: 4.5 mm, total bundle length: 2 m). The light level was controlled by adjusting the amplitude of a 1.2 kHz (402 nm LED) or 1.6 kHz (505 nm LED) square-wave modulated LED driver signal from a Stanford Research SR-830DSP lock in amplifier. Irradiance at the sample was set at 6 (402 nm) or 50 (505 nm) µW/cm^2.

After sample illumination, MB-301 and MB-404 fluorescence emission was collected by the other fiber bundle bifurcation and collimated (Newport Corp., Model 77645). MB-301 fluorescence was diverted 90˚ via a 567 nm long-pass dichroic mirror (ThorLabs DMLP567), passed through a 488 nm long-pass filter (Semrock LP02-488RE-25), a 15 nm bandpass filter centered at 540 nm (Semrock FF01-540/15-25), and detected by a Hamamatsu H7827-011 photomultiplier tube (PMT) with built-in amplifier. The MB-404 fluorescence passed through the 567 nm long-pass dichroic mirror, a 532nm long-pass filter (Semrock LP03-532RE-25), a 40 nm bandpass filter centered at 593 nm (Semrock FF01-593/40), and was detected by a Hamamatsu H7827-001 photomultiplier tube (PMT) with built-in amplifier. PMTs were powered by an Aligent E3630A power supply, and gains were adjusted via an inline potentiostat. Each amplified PMT output was synchronously detected by a lock-in amplifier (Stanford Research, SR830DSP), referenced to its respective source LED modulation frequency. Each lock-in amplifier output was read, displayed, and saved using a custom software interface. Data (raw fluorescence intensity) were read, displayed, and immediately saved by the software at a rate of 1 Hz.

3. FLUORESCENCE MEASUREMENT DATA ANALYSIS

Transdermal fluorescence was measured from both MB-404 and MB-301 as a function of time, and the baseline autofluorescence was post-processed subtracted. Since the quantum yields of these two molecules are different, and the efficiencies of each of the four probes are different, a calibration of concentration was performed using solutions of both agents in 1% intralipid in PBS as a mimic for skin. An example is shown in Figure 4.

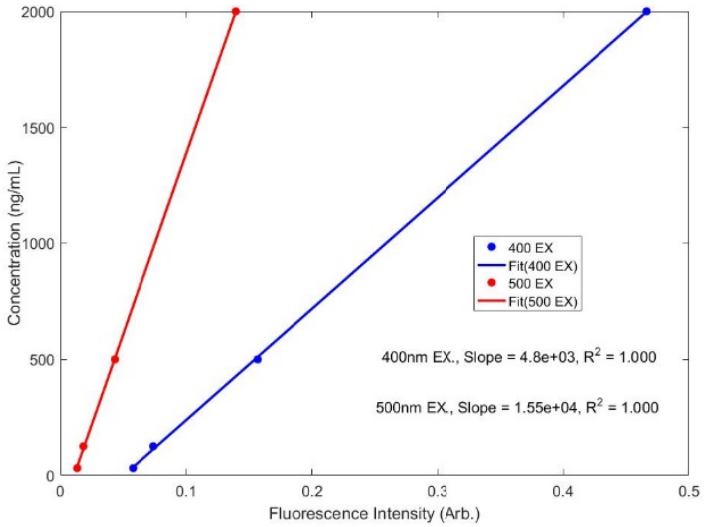

Figure 4. Calibration of MB-404 and MB-301 in 1% intralipid.

Using this calibration, the fluorescent intensities were converted to molar concentrations, the ratio of the molar concentrations was then calculated as a function of time, and the area under the curve (AUC) was deduced as a function of time.

4. RESULTS

The AUC graph in Figure 5 shows a clear delineation between indomethacin-treated rats and the control rats.

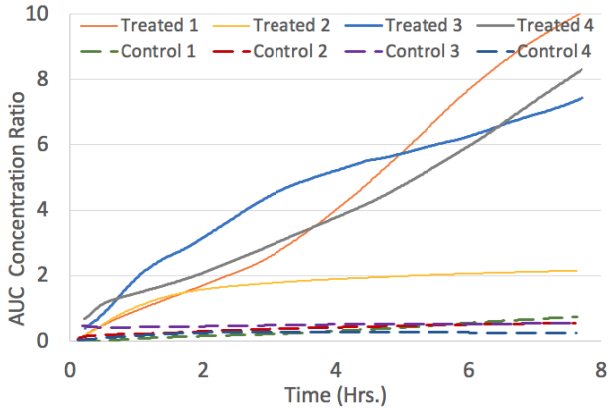

Figure 5. MB-404 to MB-301 AUC concentration ratio as a function of time.

5. CONCLUSIONS

Differentiation in the transdermal fluorescence of the ratio of two fluorophores between injury and control in an animal model of gastrointestinal permeability injury was demonstrated.

6. ACKNOWLEDGMENTS

This work was supported by a Phase II Grand Challenges Exploration Grant from the Bill & Melinda Gates Foundation to Washington University in St. Louis School of Medicine, with a sub-contract to MediBeacon Inc. Dr. Tarr is supported by NIH core grant P30DK052574.

7. REFERENCES

[1] Michielan, A. & D'Inca, R. "Intestinal Permeability in Inflammatory Bowel Disease: Pathogenesis, Clinical Evaluation, and Therapy of Leaky Gut," Mediators of Inflammation 628157 (2015).

[2] Johansson, J. E. & Ekman, T. "Gut toxicity during hemopoietic stem cell transplantation may predict acute graft-versus-host disease severity in patients," Digestive Diseases and Sciences 52, 2340–2345 (2007).

[3] Luther, J. et al. "Hepatic Injury in Nonalcoholic Steatohepatitis Contributes to Altered Intestinal Permeability," Cell Mol Gastroenterol Hepatol **1**, 222–232 (2015).

[4] Nier, A., Engstler AJ, Maier IB, Bergheim I. "Markers of intestinal permeability are already altered in early stages of non-alcoholic fatty liver disease: Studies in children," PLoS One. 2017 Sep 7;12(9):e0183282. doi: 10.1371/journal.pone.0183282. PMID 28880885.

[5] Fotis L, Shaikh N, Baszis KW, Samson CM, Lev-Tzion R French AR, Tarr PI. "Serologic Evidence of Gut-driven Systemic Inflammation in Juvenile Idiopathic Arthritis," J Rheumatol. 2017 Nov; 44(11):1624-1631. doi: 10.3899/jrheum.161589. Epub 2017 Sep 15. PMID 28916545.

[6] Denno, D. M. et al. "Use of the lactulose to mannitol ratio to evaluate childhood environmental enteric dysfunction: a systematic review," Clinical infectious diseases: an official publication of the Infectious Diseases Society of America 59 (Suppl 4), S213–219 (2014).

[7] Sequeira, I. R., Lentle, R. G., Kruger, M. C. & Hurst, R. D. "Standardising the lactulose mannitol test of gut permeability to minimise error and promote comparability," PloS One 9(6) 2014 Jun 5 doi: 10.1371/journal.pone.0099256.

[8] Lostia, A. M. et al. "A liquid chromatography/mass spectrometry method for the evaluation of intestinal permeability," Clinical biochemistry 41, 887–892 (2008).

[9] Lee, G. O. et al. "Lactulose: mannitol diagnostic test by HPLC and LC-MSMS platforms: considerations for field studies of intestinal barrier function and environmental enteropathy," Journal of Pediatric Gastroenterology and Nutrition 59, 544–550 (2014).

[10] Denno DM, VanBuskirk K, Nelson ZC, Musser CA, Hay Burgess DC, Tarr PI. "Use of the lactulose to mannitol ratio to evaluate childhood environmental enteric dysfunction: a systematic review," Clin Infect Dis. 2014 Nov 1, 59 Suppl 4:S213-9. doi: 10.1093/cid/ciu541 PMID:25305289.

[11] Dorshow RB, Hall-Moore C, Shaikh N, Talcott MR, Faubion WA, Rogers TE, Shieh JJ, Debreczeny MP, Johnson JR, Dyer RB, Singh RJ, Tarr PI. "Measurement of gut permeability using fluorescent tracer agent technology," Sci Rep. 7, 10888 (2017 Sep 7). doi: 10.1038/s41598-017-09971-y. PMID:28883476.

[12] Shirai,K.; Yanagisawa, A.;Takahashi,H.; Fukunishi, K.;Matsuoka, M. "Synthesis and fluorescent properties of 2,5-diamino-3,6-dicyanopyrazine dyes," Dyes Pigm, 39, 49–68 (1998). Compound 10.

[13] Rajagopalan, R, Neumann, WL, Poreddy, AR, Fitch, RM, Freskos, JN, Asmelash, B, Gaston, KR, Galen, KP, Shieh, JJ, Dorshow, RB. "Hydrophilic Pyrazine Dyes as Exogenous Fluorescent Tracer Agents for Real-Time Point-of-Care Measurement of Glomerular Filtration Rate," J. Med. Chem. 2011, 54, 5048–5058, dx.doi.org/10.1021/jm200257k.